

Numerical simulation of channelization by seepage erosion

Adichai PORNPROMMIN*, Yoshihiro TAKEI** Atinkut Mezgebu WUBNEH***,
and Norihiro IZUMI****

*D.Eng., Assistant Professor, Dept. Water Resources Eng., Kasetsart Univ.
(Jatujak, Bangkok, Thailand 10900)

**B.Eng., Master Student, Dept. Civil Eng., Hokkaido Univ.

***M.Sc., Doctoral Student, Dept. Civil Eng., Hokkaido Univ.

****Ph.D., Professor, Dept. Civil Eng., Hokkaido Univ.

(Kita-ku, Sapporo, Hokkaido 060-8628)

Seepage has been accepted as an important factor of rill, gully and streambank erosion in sediments. Channels initiated by seepage erosion has steep-sided walls that make it possible to investigate channel formation by the planimetric outlines of channels. We performed the numerical simulation to investigate channelization by seepage erosion based on the planimetric outlines with the use of the Dupuit-Forchheimer equation and a description of the retreat of seepage front. The retreat speed was assumed to be a power law function of the specific discharge at the front. In addition, we included the amplification coefficient in the function, which relates to the front shapes. It is hypothesized that the retreat speed is enhanced and retarded by the convexity and concavity of the fronts. The amplification coefficient is used to represent the physically based diffusion process of seepage erosion. As expected, the incipient channel spacing in the simulations without the effect of the front shapes depend on the numerical diffusion, which depends on the scale of grid size. Including the effect of the front shapes, the characteristic incipient channel spacing can be estimated. The results of the simulations are found to be consistent with the existing linear stability analysis.

Key Words : *channelization, seepage erosion, numerical simulation*

1. Introduction

Many geomorphological features show self-organized patterns with uniform spacing from micro-scale bedforms (ripples and dunes) to mountain ranges (ridges and valleys)¹⁾. In soil-mantled landscapes, uniform spacing is especially apparent among first-order drainage basins in both field and laboratory studies^{2),3),4)}. Bull and Kirkby⁵⁾ listed the processes affecting gully and channel morphology as overland flow, hillslope infilling, pipe initiation, pipe enlargement by flow, mass failures and the magnitude of storm events. They mentioned that there are gaps in the understanding of mass failures and channel network formation by seepage erosion. Chu-Agor et al.⁶⁾ conducted experiments in a 50-cm wide chamber in order to study headcut formation in detail. They proposed that seepage can cause hillslope instability through three different mechanisms: an increase in soil pore-water pressure, seepage gradient forces, and seepage particle mobilization and undercutting. However, as seepage erosion is generated by the

complex interaction between seepage and other mechanisms, the roles of seepage on slope instability and channelization are not fully understood.

In the theoretical viewpoint, the inception of channelization by seepage erosion have been much less developed than that by overland flow. In the case of channelization by overland flow, one of the first studies was conducted by Smith and Bretherton⁷⁾. In their analysis, a tilted plateau was imposed by a small amplitude of laterally perturbed wave. Although the predicted spacing between channels was found to be infinitely small because of the steady uniform open channel flow assumption, their groundbreaking work has served to motivate many later studies. Nowadays the theory has been advanced that channelization by overland flow can be tackled by using sophisticated linear stability analysis, in which the finite characteristic incipient channel spacing can be determined by the growth rate of perturbations^{8),9),10)}. In the case of channelization by seepage erosion, Schorghofer et al.⁴⁾ did numerical simulations of groundwater flow and proposed that small deformations of groundwa-

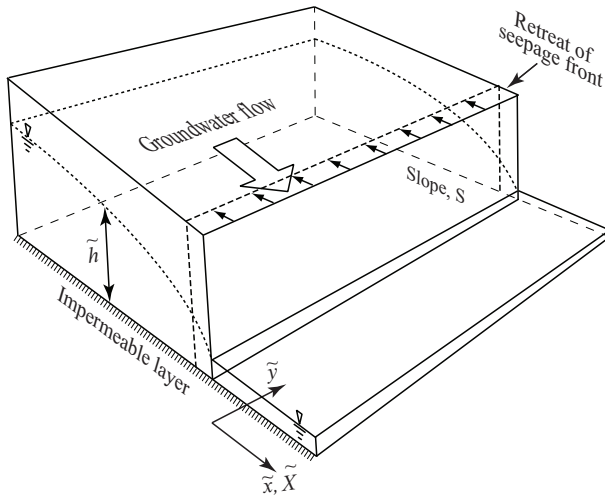


Fig. 1 Conceptual diagram of a sediment layer with groundwater flow and the retreat of seepage front.

ter table amplify groundwater flux into channels and lead to further growth of channels. They concluded that channel spacing is a function of channel length and coarsens with time because of an extension of channel length. However, they cannot find the finite characteristic incipient channel spacing.

Recently, Pornprommin and Izumi¹¹⁾ performed the first linear stability analysis of channelization by seepage erosion. The analysis is based on the planimetric outlines of channels with the use of the Dupuit-Forchheimer equation for groundwater flow model and a description of the retreat of seepage front for channel evolution by seepage erosion. The retreat speed consists of two terms. The first term is a power law function of the specific discharge at the front exceeding a critical discharge. The second term is a diffusion-like function of the front shapes, in which the retreat speed is enhanced and retarded by the convexity and concavity of the fronts, respectively. They found that the characteristic incipient channel spacing becomes infinitely small if the effect of the front shapes is excluded. With the use of the experimental results of plastic pellet sediment¹²⁾, they found that the normalized diffusion-like coefficient is the order of 0.1. In this study, based on their theoretical study, we perform numerical simulations to investigate the characteristics of channelization by seepage erosion.

2. Formulation

2.1 Groundwater model

Let us consider groundwater flow in an unconfined aquifer with free water surface above an inclined impermeable layer as shown in Figure 1. Similar to other models of landscape evolution due to seepage erosion^{13),14),15)}, the Dupuit-Forchheimer equation is

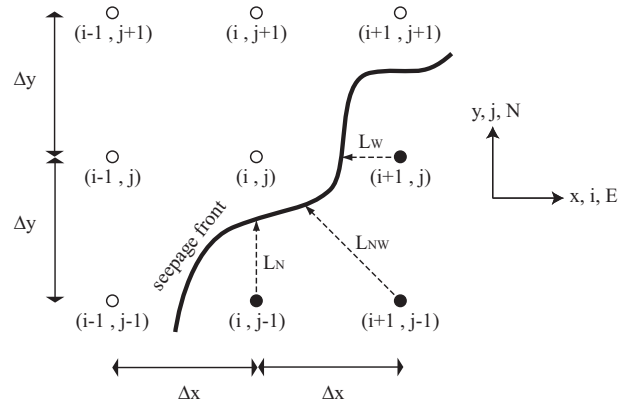


Fig. 2 Grid layout for the numerical computation where the nodes with open dot mean uneroded area, the nodes with solid dot mean eroded area, and the vectors L are used for detecting the locations of seepage front.

employed to describe the movement of groundwater flow in this study, such that

$$\frac{1}{\phi} \frac{\partial h}{\partial t} - \frac{\partial}{\partial x} \left[Kh \left(\frac{\partial h}{\partial x} - S \right) \right] - \frac{\partial}{\partial y} \left(Kh \frac{\partial h}{\partial y} \right) = R \quad (1)$$

where t is time, x and y are the streamwise and lateral directions respectively, h is water depth, K is the hydraulic conductivity, ϕ is porosity, S is the slope of the impermeable layer, and R is the recharge or withdrawal rates (positive or negative values) of groundwater from the surface.

In Figure 1, groundwater with a constant water depth at the upstream end is assumed to flow through the sediment layer and emerges at the downstream end, whereas the left and right banks are assumed to be walls. At the downstream end where seepage front is located, if groundwater depth is zero, the velocity, however, becomes infinity in the Dupuit approximation, in which it will violate our model. Thus, a constant non-zero value of water depth is necessary to be assumed at seepage front in our model. Then seepage erosion can be initiated if seepage flow is sufficiently high. Seepage erosion causes mass failures and the retreat of seepage front. As a result, channelization can be observed if the retreat of seepage front is not laterally uniform.

With the use of the finite difference method, we discretized (1). In order to increase the accuracy of the computation in the vicinity of seepage front when the front is not located exactly at the computed nodes, we introduce 8 vectors directing to the 8 directions (N, NE, E, SE, S, SW, W and NW) as shown in Figure 2. If seepage front is detected to be between the computing node (i, j) and the surrounding nodes $(i \pm 1, j \pm 1)$, the vectors are used to express the locations of the front. We employed the fully implicit discretization with the central scheme as described by Patankar¹⁶⁾.

Thus, the discretization equation of the groundwater flow equation (1) is

$$a_P h_P = a_E h_E + a_W h_W + a_N h_N + a_S h_S + a_P^0 h_P^0 + b_P \quad (2)$$

where the subscript P denotes the computing node, the subscripts E , W , N and S denote the adjacent nodes in the east, west, north and south of the computing node respectively, the superscript 0 denotes the present time, and a_P , a_P^0 , a_E , a_W , a_N , a_S and b_P are the coefficients, such that

$$a_P = a_P^0 + a_E + a_W + a_N + a_S \quad (3a)$$

$$a_P^0 = \frac{1}{\phi_P \Delta t} \quad (3b)$$

$$(a_E, a_W) = \left(\frac{T_E}{\Delta x_P \Delta x_E}, \frac{T_W}{\Delta x_P \Delta x_W} \right) \quad (3c, d)$$

$$(a_N, a_S) = \left(\frac{T_N}{\Delta y_P \Delta y_N}, \frac{T_S}{\Delta y_P \Delta y_S} \right) \quad (3e, f)$$

$$b_P = R_P - \frac{T_E S}{\Delta x_P} + \frac{T_W S}{\Delta x_P} \quad (3g)$$

where Δt denotes time step, Δx and Δy are the x and y direction distances between two adjacent grid points, and T denotes the multiplication between the hydraulic conductivity K and water depth h .

2.2 Front propagation model

In the theoretical analysis of Pornprommin and Izumi¹¹), the retreat speed of seepage front in the x direction is assumed to be described as follows:

$$\frac{\partial X}{\partial t} = -\alpha \left(\frac{q_{x=X} - q_{th}}{q_r} \right)^\gamma \cos \theta + \epsilon \frac{\partial^2 X}{\partial y^2} \quad (4)$$

where X denotes the x -direction distance of seepage front from the y axis, $q_{x=X}$, q_{th} and q_r are the unit discharge at seepage front, the threshold unit discharge and the reference unit discharge respectively, α is the coefficient with the dimension of velocity, γ is an exponent, ϵ is the diffusion-like coefficient with the dimension of Length²/Time, and θ is the angle between the direction normal to seepage front and the x axis. Thus,

$$\cos \theta = \frac{1}{\sqrt{1 + (\partial X / \partial y)^2}} \quad (5)$$

In (4), the retreat speed of seepage front is assumed to consist of two terms. The first term on the right side of (4) is expressed as a power law function of

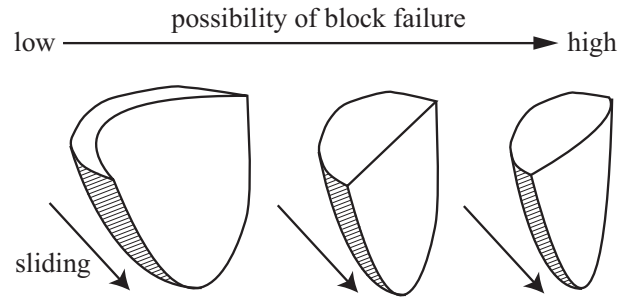


Fig. 3 Hypothesis of the effect of the curvature of seepage front on the possibility of block failure. Shaded area shows the failure surface.

groundwater flow exceeding the threshold value proposed by Howard and McLane¹⁷), and, according to the experiments by Fox et al.¹⁸), the exponent γ is between 1 and 1.6. In addition, the first term is set to be zero if $q_{x=X} \leq q_{th}$. The second term on the right side of (4) is expressed as a diffusion-like function of the seepage front shapes, in which the retreat speed is enhanced and retarded by the convexity and concavity of the fronts, respectively. This hypothesis was firstly proposed by Howard¹⁴), and it can be simply explained in Figure 3. The sediment blocks with the concave, linear and convex outlines of seepage front are shown at the left, center and right of the figure, respectively. These three types of sediment blocks with the same volume but different in shapes are considered to slide down. As the shape of each block differs, the failure surface area of each block also differs. It is hypothesized that the failure surface area of the block should become smaller if the convexity of the failure block increases, and thus it induces a higher possibility of failure. According to the authors' knowledge, however, no study has clearly proposed a function to handle the effect of seepage front shapes on the retreat speed of the front. Thus, the proposed second term on the right side of (4) representing the effect of the front shapes is unclear whether it behaves according to the real phenomenon. Moreover, we found one important disadvantage of applying (4) for the retreat speed of seepage front. Supposed that the front has a sufficiently strong concave shape, and the second term affects the retreat speed of the front stronger than the first term, which is a function of unit discharge, it is possible that the front will not be retreated but advanced downstream (deposition) because the second term in (4) is independent from the first term. However, this possibility that deposition can occur is inappropriate in the present case of the erosional phenomenon.

In this study, we propose another form of the retreat speed function as follows:

$$\frac{\partial L_m}{\partial t} = \alpha \Gamma \left[\frac{q_m - q_{th}}{q_r} \right]^\gamma \quad (6)$$

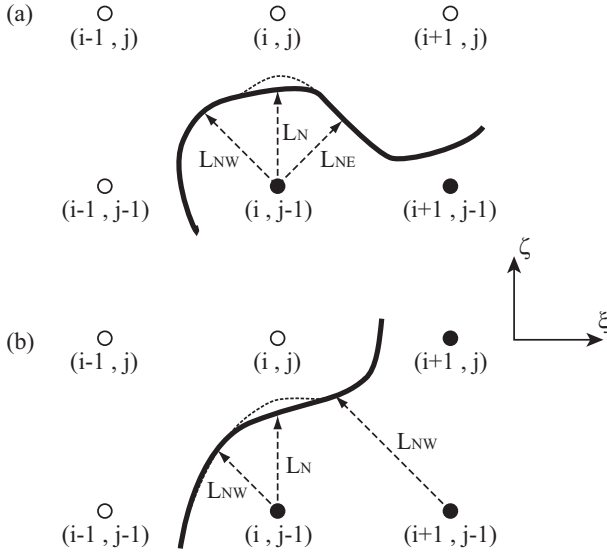


Fig. 4 Concept of computing the front shapes by using three points for the retreat speed of L_N of the node $(i, j-1)$, where (a) the case that the node $(i+1, j)$ is uneroded area, and (b) the case that the node $(i+1, j)$ is eroded area.

where the subscript m denotes the computing vector direction (N, NE, E, SE, S, SW, W and NW), L_m is the length of the vector m , q_m is the unit discharge in the m direction, and the amplification coefficient Γ is assumed to be

$$\Gamma = 1 - \beta \frac{\partial^2 \xi_m}{\partial \zeta_m^2} \Big/ \sqrt{a^2 + \left(\frac{\partial^2 \xi_m}{\partial \zeta_m^2} \right)^2} \quad (7)$$

where ζ and ξ denote the axes normal and parallel to the m direction respectively, β is the coefficient (0 to 1) associating with the maximum magnitude of Γ , and a is the coefficient (0 to ∞) representing the steepness of the function Γ . As $\partial^2 \xi_m / \partial \zeta_m^2$ ranges between $-\infty$ and ∞ , the amplification function Γ ranges between $1 + \beta$ and $1 - \beta$.

With the use of the retreat speed function (6), it will prevent the possibility that deposition can occur in the simulation. In addition, if (6) is expanded by the perturbation method, the coefficient a in (7) can relate to the diffusion-like coefficient ϵ in (4) in the linear stability analysis as follows:

$$\epsilon^* = \frac{(1 - \psi)^\gamma}{a} \quad (8)$$

where ϵ^* is the normalized diffusion-like coefficient and found to be in the order of 0.1 from the previous analysis¹¹), and ψ denotes the ratio between the threshold discharge for erosion and the reference discharge (q_{th}/q_r). Thus, a is approximately in the order of 1 to 10.

Figure 4 show the concept of computing the convexity and concavity of the fronts in this study by using

Table 1 Simulation conditions.

no.	1	2	3	4	5
ψ	0.3				
S	0				
R	0				
K	0.1 m/s (random)				
upstream h	0.073 m				
downstream h	0.002 m				
width x length	1.5 m x 1.2 m				
Δt	0.1 s				
$\Delta x, \Delta y$ (m)	0.03		0.01	0.03	0.01
α	1 cm/min				
γ	1				
q_r	0.00222 m ² /s				
q_{th}	0	0.001 m ² /s			
β	-			0.95	
a	-			1	

three points. Two examples for calculating $\partial^2 \xi_m / \partial \zeta_m^2$ for the retreat speed of L_N of the node $(i, j-1)$ are shown. In Figure 4a, three points are located by the vectors L_{NW} , L_N and L_{NE} of the node $(i, j-1)$ because the nodes $(i-1, j)$ and $(i+1, j)$ are uneroded area, whereas the vector L_{NE} of the node $(i, j-1)$ is replaced by the vector L_{NW} of the node $(i+1, j-1)$ in Figure 4b because the node $(i+1, j)$ is eroded area.

3. Simulation conditions

Table 1 shows five cases of our numerical simulation. To provide perturbations in the simulation, we imposed a random function to the hydraulic conductivity K . However, the averaged value of K is equal to 0.1 m/s in every case. The domain of our simulation is 1.5 m wide and 1.2 m long. The distances Δx and Δy in the simulation no.1, 2 and 4 are 0.03 m, whereas they are 0.01 m in the simulation no.3 and 5. Thus, the total nodes in the simulation no.1, 2 and 4 are 51 x 40, and the total nodes in the simulation no.3 and 5 are 151 x 121. The threshold unit discharge for erosion q_{th} is set to be 0.001 m²/s except in the simulation no.1, in which $q_{th} = 0$. The simulations no.1–3 do not consider the effect of the front shapes on the retreat speed of the front, whereas the simulations no.4 and 5 consider the effect using (6) and (7). Thus, the effects of the threshold discharge q_{th} , grid distances Δx and Δy and front shapes Γ on the formation of channels by seepage erosion are studied by these five cases of numerical simulations.

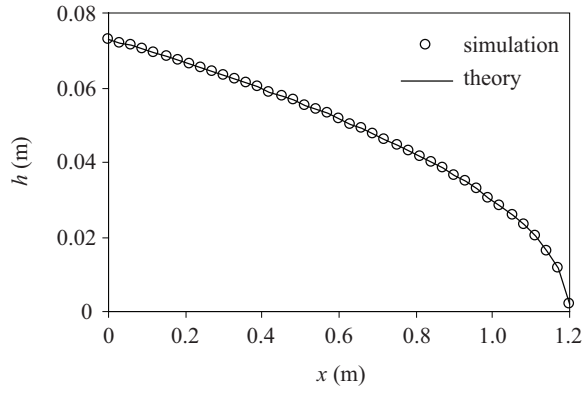


Fig. 5 Comparison of groundwater depth along the streamwise direction between the simulation and the theory.

4. Results and discussion

4.1 Streamwise groundwater profile

Figure 5 shows the comparison of the streamwise groundwater depth between the simulation and the theory. In the theory, the relation between the streamwise distance x and groundwater depth h is

$$\frac{h_{U/S}^2 - h^2}{h_{U/S}^2 - h_{D/S}^2} = \frac{x}{L_0} \quad (9)$$

where $h_{U/S}$ and $h_{D/S}$ are groundwater depths at the upstream and downstream of the domain respectively, and L_0 is the domain length. It is found that groundwater depth decreases in the parabolic form, and the numerical model can simulate the groundwater depth accurately.

4.2 Channel evolution

Figure 6 shows the plan view of channel evolution of the simulation no.1. The groundwater flow is from the left to the right of the figure. The lines show the position of the outlines of channels at intervals of 300 s from 0 to 1800 s. At $t=300$ s, it is found that all parts of seepage front retreat because the threshold discharge q_{th} is set to be zero. However, we can find some parts of the front retreat faster than others because the random function was imposed to the hydraulic conductivity K and causes an increase in groundwater in some parts of the front. As time progresses, the parts that initially retreated faster migrate upstream continuously at faster speeds, and many channels can be clearly observed because of the deviation of the locations of seepage fronts. As groundwater flow generally concentrates at the parts of the front that are closer to the upstream (channel heads), an increase in water discharge at that part of the front results in an increase in the retreat speed of that part, and finally the front cannot maintain

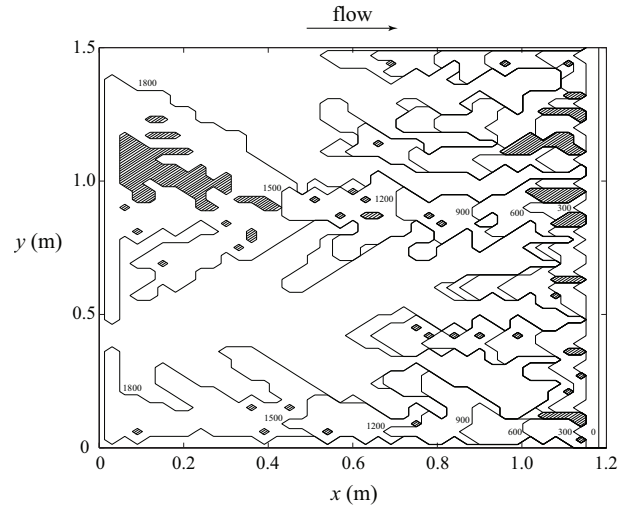


Fig. 6 Plan view of channel evolution of the simulation no.1. The lines show the position of the outlines of channels at intervals of 300 s from 0 to 1800 s. The shaded areas denote uneroded islands surrounding by eroded areas.

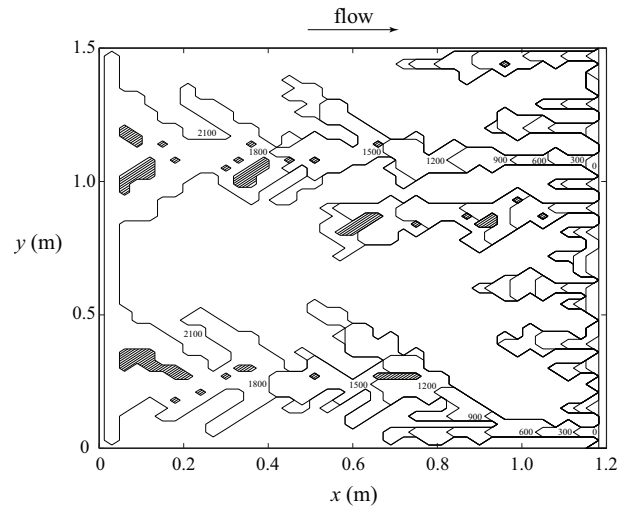


Fig. 7 Plan view of channel evolution of the simulation no.2. The lines show the position of the outlines of channels at intervals of 300 s from 0 to 2100 s. The shaded areas denote uneroded islands surrounding by eroded areas.

the laterally uniform retreat. At $t=1800$ s, the channels already reached the upstream end of the simulated domain, and we can find six main channels, in which some channels were bifurcated into more than two channels. In addition, many small islands shown by shaded areas in the figure can be found in the simulation no.1.

The channel evolution of the simulation no.2 is shown in Figure 7. The simulations no.1 and 2 differ on the threshold discharge q_{th} . While $q_{th} = 0$ in

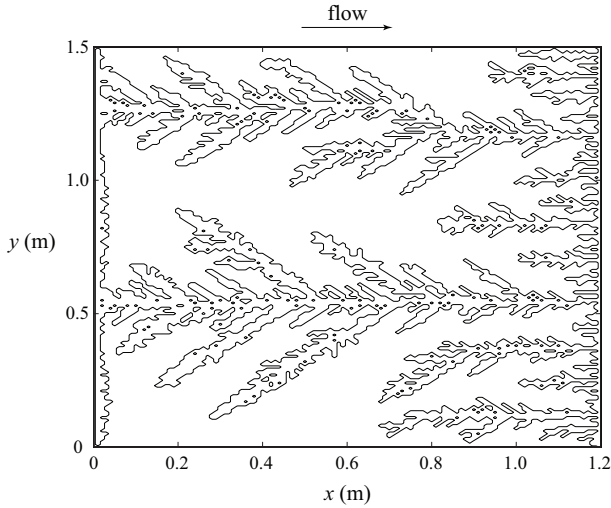


Fig. 8 Plan view of channel evolution of the simulation no.3. The line show the position of the outlines of channels at 1500 s.

the simulation no.1, $q_{th} = 0.001\text{m}^2/\text{s}$ in the simulation no.2. Thus, the effect of the threshold discharge q_{th} is investigated by comparing the results of two cases. Although the characteristics of channel evolution in both cases are commonly identical, some difference can be observed. In the simulation no.2, channel widths are smaller than those in the simulation no.1, and it took longer time (2100 s) for the retreat of seepage front to reach the upstream end. Also some small islands shown by shaded areas can be found in this simulation, and approximately 12 channels were observed at the end of the simulation.

Figure 8 shows the result of the simulation no.3 at $t=1500$ s. The grid sizes Δx and Δy in the simulation no.3 is equal to 0.01 m finer than those in the two previous simulations of 0.03 m. We found a very different result in this simulation. Channel widths become much smaller, many channel bifurcations are found, and the number of channels is about 3 times of the number in the simulation no.2. According to the linear stability analysis by Pornprommin and Izumi¹¹⁾, the characteristic channel spacing becomes infinitely small if the effect of the front shapes is excluded. The results of the numerical simulations are consistent with the finding in the linear theory. As the simulations no.1–3 do not include the effect of the front shapes, the channel spacing becomes smaller when grid size reduces because of the change in the numerical diffusion. It is known that the numerical diffusion depends on the scale of grid size. This shortcoming was also observed by Howard¹³⁾. According to Perron et al.¹⁾, models of long-term landscape evolution commonly consist of advective erosion processes (e.g., stream incision) and diffusion-like mass transport (e.g., soil creep), and the first-order valley spacing is more sensitive to the process competition

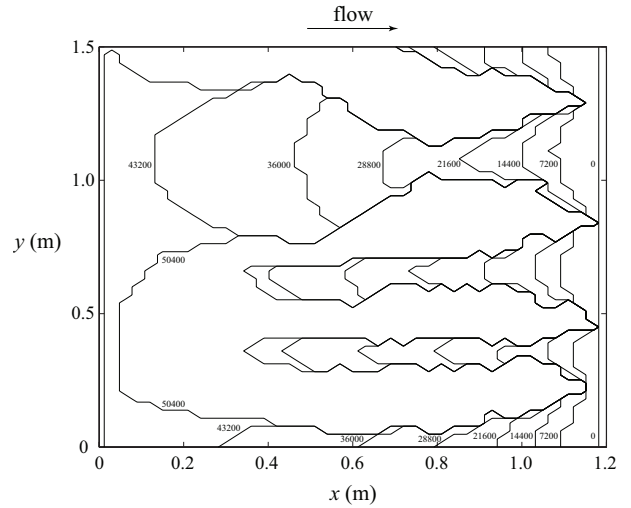


Fig. 9 Plan view of channel evolution of the simulation no.4. The lines show the position of the outlines of channels at intervals of 7200 s from 0 to 50400 s.

than the magnitude of a threshold erosion. Although the present model differs from the common models of long-term landscape evolution, the results show that the physically based diffusion process is also necessary for simulating the characteristic incipient channel spacing in the present model.

Figure 9 shows the plan view of channel evolution of the simulation no.4. Unlike the simulations no.1–3, the simulation no.4 included the effect of the front shapes. Again the results drastically change from the results of the three previous simulations. The retreat speed of the front is much slower than the previous simulations that the lines in Figure 9 show the position of the outlines of channels at intervals of 7200 s from 0 to 50400 s. We found five main channels with similar sizes. At the beginning, these 5 channels seem to migrate upstream with approximately same speed. However, at $t=28800$ s the second channel from the left bank, in which its channel head was nearest to the upstream end, started to expand its width. Then the second channel has a distinctive light-bulb shape as time progresses. This shape was found in the experiments by Kochel and Piper¹⁹⁾, when the channels tapped the perched aquifer that causes the acceleration of groundwater discharge, and it also found in the experiments of Pornprommin and Izumi¹²⁾, when the chamber slope is sufficiently small. In our simulations, the upstream boundary is a constant groundwater depth, which implies that the discharge will increase when the seepage front retreats. Since the second channel from the left bank can retreat faster than other channels, accelerated groundwater discharge may concentrate to that channel, and, with the flat slope ($S = 0$) that causes large difference in water depths at upstream end and at the front, the

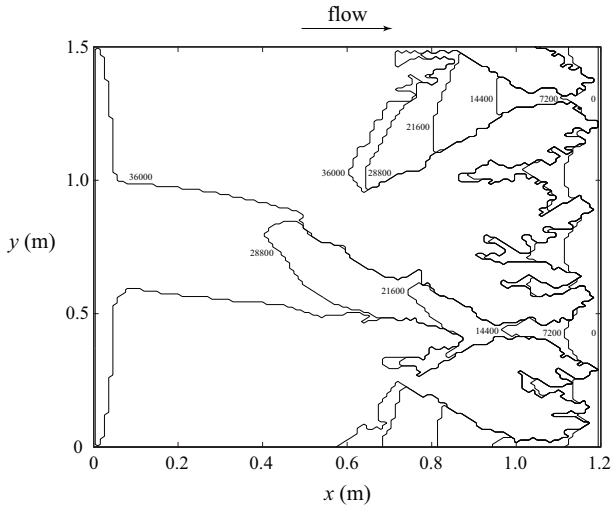


Fig. 10 Plan view of channel evolution of the simulation no.5. The lines show the position of the outlines of channels at intervals of 7200 s from 0 to 36000 s.

flow concentration may increase at a faster rate, and finally it results in the light-bulb shape. However, this light-bulb shape cannot be found in the previous simulations that exclude the effect of the front shapes. Thus, the effect of the front shapes may be one of the causes of lateral widening in the simulation no.4.

Figure 10 shows the result of our last simulation. In the simulation no.5, the effect of the front shapes was included, but Δx and Δy are 0.01 m finer than those in the simulation no.4. The lines show the position of the outlines of channels at intervals of 7200 s from 0 to 36000 s. At the beginning period $t=7200$ s, the seepage front form a systematic sinusoidal shape similar to that appears in the simulation no.4. In addition, the number of channels in this simulation is comparable to the number in the previous simulation. In the simulations no.2 and 3, in which Δx and Δy decrease into one third, the number of channels in the simulation no.3 drastically increases and was around 3 times of the number in the simulation no.2. Thus, with the effect of the front shapes, we found that the simulation can qualitatively maintain the number of incipient channels. On the other hand, the characteristic incipient channel spacing can be observed if the effect of the front shapes, the physically based diffusion process, is employed. This is consistent to the existing linear stability analysis¹¹⁾. As time progresses, however, it is found that some of these seven main channels cannot maintain their forms and bifurcate into many sub-channels. Sub-channels are very small and have the width of only one grid size, which is the same size as channels in the simulation no.3, in which Δx and Δy are also 0.01 m. It implies that in the present study the effect of the front shapes may be sufficient in the beginning period of the simulations,

but it cannot maintain as time progresses. The results show that the long-term channel evolution partially depends on the scale of grid size in the simulation no.5. We hypothesized that the present techniques to estimate the retreat of seepage front by 8-vectors method and to compute the effect of the front shapes by three-points method may be not accurate enough. It will be investigated in more details, and other techniques may be used in the future.

5. Conclusion

The numerical simulations of channelization by seepage erosion are performed with the use of the Dupuit-Forchheimer equation as the groundwater flow equation and a description of the retreat of seepage front as the channel evolution model. With the use of 8 vectors in 8 directions (N, NE, E, SE, S, SW, W, NW), the locations of seepage front between grid points can be detected. In the description of the retreat of the front, the retreat speed is assumed to be a power law function of the specific discharge at the front exceeding a critical discharge. In addition, we included the amplification coefficient in the retreat speed function, in which the coefficient represents the effect of the front shapes on the retreat speed. If the front has a convex shape, the possibility of mass failure becomes higher, and, correspondingly, the magnitude of the coefficient increases. In this study, the front shapes was estimated by the three-points method, in which the second derivative term of seepage front was calculated by three points detected by three vectors. From the results of the simulations, it is found that, excluding the effect of the front shapes, the characteristic incipient channel spacing cannot be found, and the spacing depends on the numerical diffusion, which relates to the scale of grid size. Thus, as the grid size becomes finer, the spacing becomes smaller. The present result is consistent with the analyses by Pornprommin and Izumi¹¹⁾ and Howard¹³⁾. Including the effect of the front shapes, we found that the characteristic incipient channel spacing can be qualitatively estimated. However, when channels develop further, they divides into several sub-channels with the sizes that relates to the scale of grid size. Thus, it implies that at present our model can explain the inception of channels, but it is not sufficient enough to simulate the long-term channel evolution. This should be improved in the future.

Acknowledgement

This study was supported by Hokkaido River Disaster Prevention Research Center and the Japan Society for the Promotion of Science Postdoctoral Fellowship Program (grant-in-aid P 07116).

REFERENCES

- 1) Perron, J. T., W. E. Dietrich and J. W. Kirchner: Controls on the spacing of first-order valleys, *J. Geophys. Res.*, Vol. 113, F04016, doi:10.1029/2007JF000977, 2008.
- 2) Montgomery, D. R. and W. E. Dietrich: Channel initiation and the problem of land landscape scale, *Science*, Vol. 255(5046), pp. 826–830, 1992.
- 3) Perron, J. T., J. W. Kirchner and W. E. Dietrich: Spectral signatures of characteristic spatial scales and nonfractal structure in landscapes, *J. Geophys. Res.*, Vol. 113, F04003, doi:10.1029/2007JF000866, 2008.
- 4) Schorghofer, N., B. Jensen, A. Kudrolli and D. H. Rothman: Spontaneous channelization in permeable ground: theory, experiment, and observation, *J. Fluid Mech.*, Vol. 503, pp. 357–374, 2004.
- 5) Bull, L. J. and M. J. Kirkby: Gully processes and modelling, *Prog. Phys. Geog.*, Vol. 21(3), pp. 354–374, 1997.
- 6) Chu-Agor, M., G. A. Fox, R. M. Cancienne and G. V. Wilson: Seepage caused tension failures and erosion undercutting of hillslopes, *J. Hydrol.*, Vol. 359, pp. 247–259, 2008.
- 7) Smith, T. R. and F. P. Bretherton: Stability and the conservation of mass in drainage basin evolution, *Water Resour. Res.*, Vol. 8(6), pp. 1506–1529, 1972.
- 8) Izumi, N. and G. Parker: Linear stability analysis of channel inception: downstream-driven theory, *J. Fluid Mech.*, Vol. 419, pp. 239–262, 2000.
- 9) Izumi, N. and K. Fujii: Channelization on plateaus composed of weakly cohesive fine sediment, *J. Geophys. Res.*, Vol. 111, F01012, doi:10.1029/2005JF000345, 2006.
- 10) Pornprommin, A., N. Izumi and T. Tsujimoto: Channelization on plateaus with arbitrary shapes, *J. Geophys. Res.*, Vol. 114, F01032, doi:10.1029/2008JF001034, 2009.
- 11) Pornprommin, A. and N. Izumi: Linear stability analysis of escarpment planforms by groundwater sapping, *Annual Journal of Hydraulic Engineering*, Vol. 53, *JSCE*, pp. 139–144, 2009.
- 12) Pornprommin, A. and N. Izumi: Experimental study of channelization by seepage erosion, *J. Applied Mechanics*, Vol. 11, *JSCE*, pp. 709–717, 2008.
- 13) Howard, A. D.: Groundwater Sapping Experiments and Modeling, in *Sapping Features of the Colorado Plateau: A Comparative Planetary Geology Field Guide*, edited by A. D. Howard, R. C. Kochel, and H. Holt, *NASA Spec. Publ.*, SP-491, pp. 71-83, 1988.
- 14) Howard, A. D.: Simulation modeling and statistical classification of escarpment planforms, *Geomorphology*, Vol. 12, pp. 187–214, 1995.
- 15) Luo, W. and A. D. Howard: Computer simulation of the role of groundwater seepage in forming Martian valley networks, *J. Geophys. Res.*, Vol. 113, E05002, doi:10.1029/2007JE002981, 2008.
- 16) Patankar, S. V.: Numerical heat transfer and fluid flow, Series in computational methods in mechanics and thermal sciences, *Hemisphere publishing corporation*, pp. 197, 1980.
- 17) Howard, A. D. and C. F. McLane: Erosion of cohesionless sediment by groundwater seepage, *Water Resour. Res.*, Vol. 24(10), pp. 1659-1674, 1988.
- 18) Fox, G. A., G. V. Wilson, R. K. Periketi and B. F. Cullum: A sediment transport model for seepage erosion of streambanks, *J. Hydraul. Eng.*, Vol. 11(6), pp. 603-611, 2006.
- 19) Kochel, R. C. and J. F. Piper: Morphology of large valleys on Hawaii: Evidence for groundwater sapping and comparisons with Martian valleys, *J. Geophys. Res., Proc. Lunar Planet Sci. Conf. 17th Part 1*, Vol. 91, suppl., pp. E175-E192, 1986.

(Received April 9, 2009)